Journal of Applied Physics

RESEARCH ARTICLE | MARCH 04 2025

Effects of nitrosyl fluoride based gas treatment on fluorination and redox reaction at GaN surface and Pt/GaN interface

Takahiro Nagata ; Asahiko Matsuda ; Takashi Teramoto ; Dominic Gerlach ; Peng Shen ; Shigenori Ueda ; Takako Kimura ; Christian Dussarrat ; Toyohiro Chikyow

J. Appl. Phys. 137, 095304 (2025)
https://doi.org/10.1063/5.0224068

AIP Publishing

Journal of Applied Physics ARTICLE pubs.aip.org/aip/jap

Effects of nitrosyl fluoride based gas treatment on fluorination and redox reaction at GaN surface and Pt/GaN interface

Cite as: J. Appl. Phys. **137**, 095304 (2025); doi: 10.1063/5.0224068
Submitted: 19 June 2024 · Accepted: 6 February 2025 ·
Published Online: 4 March 2025

Takahiro Nagata,[1,a)] Asahiko Matsuda,[2] Takashi Teramoto,[3] Dominic Gerlach,[1,b)] Peng Shen,[3] Shigenori Ueda,[1,4] Takako Kimura,[3] Christian Dussarrat,[3] and Toyohiro Chikyow[5]

AFFILIATIONS

[1]Research Center for Electronic and Optical Materials, National Institute for Materials Science (NIMS), 1-1 Namiki, Tsukuba, Ibaraki 305-0044, Japan
[2]Materials Data Platform, NIMS, 1-1 Namiki, Tsukuba, Ibaraki 305-0044, Japan
[3]K.K. Air Liquide Laboratories, 2-2 Hikarinooka, Yokosuka, Kanagawa 239-0847, Japan
[4]Synchrotron X-ray Station at SPring-8, NIMS, Sayo, Hyogo 679-5148, Japan
[5]Center for Basic Research on Materials, NIMS, Tsukuba, Ibaraki 305-0047, Japan

[a)]**Author to whom correspondence should be addressed:** NAGATA.Takahiro@nims.go.jp
[b)]**Present address:** Zernike Institute for Advanced Materials, University of Groningen, Nijenborgh 4, 9747 AG Groningen, The Netherlands.

ABSTRACT

The effects of nitrosyl fluoride (FNO) gas treatment on the surface of GaN(0001) and its interface with sputtered Pt were investigated by hard x-ray photoelectron spectroscopy (HAXPES). Annealing GaN and Pt/GaN samples in an FNO gas atmosphere resulted in the appearance of prominent F 1*s* peaks in the HAXPES spectra, indicating the efficient formation of Ga–F_x bonding states not only in bare-GaN but also in Pt/GaN, even when the FNO gas treatment was performed after Pt deposition. In addition, the chemical shifts of the Ga $2p_{3/2}$ and N 1*s* peaks corresponded to a Fermi level shift toward the valence band. The FNO gas treatment induced greater oxidation of the GaN surface than the Pt/GaN interface. By contrast, at the Pt/GaN interface, the unintentionally formed oxide GaO_x was reduced, resulting in an improvement of the electrical properties. The results of this study suggest that FNO gas treatment is an effective post-processing method for the fluorination of GaN-based systems after metal deposition.

I. INTRODUCTION

Nitride semiconductor devices are becoming increasing practical, and demand exists for even higher functionality, such as high-speed operation and higher breakdown voltages. In GaN device applications, the high density of vacancies associated with dangling bonds is one unresolved issue.[1] In Si devices, defect passivation is generally achieved by a hydrogen-based process that terminates the dangling bonds with H and removes the vacancy states.[2] However, this method is ineffective for defect passivation in GaN devices.[3–5] As an alternative to H, F has been proposed as a candidate element that can terminate the dangling bonds. F termination has been investigated with Si and Ge.[6,7] F has a high electronegativity, and it tends to form highly stable bonds. It is also expected to be useful for post-process defect passivation because of its small atomic radius and high diffusivity. The introduction of F into GaN and AlGaN/GaN devices has been studied for passivating defects, modifying defects, and altering device properties such as the threshold voltage (V_{th}).[8,9] F incorporation is typically accomplished by ion implantation,[10,11] CF_4 plasma exposure,[8,10,12] or, less commonly, annealing under an NF_3 atmosphere.[13] These methods are used in conventional Si device process technology; however, the kinetic energy in the process is high and recovery from damage requires

high-temperature heat treatment and other processes. Atomic layer etching of GaN surfaces by RF processing has also been reported recently.[14,15] Fluorination of the GaN surface and Pt/GaN interface with N_2 gas containing NF_3 has also been demonstrated;[16] however, these methods introduce additional defects into the bulk region. In the present study, to suppress the introduction of such defects and to promote weak fluorination, we used nitrosyl fluoride (FNO)-based gases.

FNO is a highly reactive fluorinating agent that converts many metals to fluorides and releases nitric oxide (NO) in the process. As a rudimentary consideration of the reaction thermodynamics, the standard heat of formation ($-\Delta H_f°$) for FNO, GaN, and fully fluorinated GaF_3 is 66, 110, and 1163 kJ/mol, respectively.[17,18] Thus, the $\Delta H_f°$ values indicate that the fluorination of FNO is the preferred reaction. We hypothesized that FNO decomposition would also be effective compared with NF_2–F bond breaking ($-\Delta H_f° = 239$ kJ/mol).[19] The dissociation energy of 192 kJ/mol for the N–F bond of nitrile fluoride (FNO_2) is ~75 kJ/mol lower than that of a typical N–F single bond.

In addition, to verify the feasibility of FNO gas treatment as a post-process dangling-bond-termination method, we fabricated Pt/GaN contacts and subjected them to post-annealing under an FNO atmosphere. To nondestructively characterize the formed interface, hard x-ray photoelectron spectroscopy (HAXPES, $h\nu = 5953.4$ eV), which has a probe depth of Pt greater than 10 nm, was employed.[20,21] The deep detection depth of HAXPES enabled direct observation of the Pt/GaN interface. We found that the detection depth could be varied by using HAXPES in conjunction with conventional soft x-ray PES (SXPES) using an Al-Kα light source ($h\nu = 1486.6$ eV).

II. EXPERIMENTAL PROCEDURES

For HAXPES electrical measurements, unintentionally doped GaN (0001) films (thickness: 4–6 μm) grown by epitaxial MOCVD on c-sapphire substrates (POWDEC) were used, with a full width at half maximum (FWHM) value of 252 arcsec in the x-ray diffraction omega-rocking curve of (0002) reflection (XRD-RC). For electrical measurements, n-type Si-doped GaN bulk crystal (Shinyo, thickness: 362 μm, resistivity <0.05 Ω cm) were used, with an FWHM value of 72 arcsec in the XRD-RC. Notably, in the HAXPES experiments, the same epitaxial GaN film used in our previous study[16] on GaN surface fluorination with NF_3 and F_2 was used so that the results could be compared. By contrast, for electrical characteristics, a vertical device structure with top and bottom electrodes formed on GaN bulk crystals was used to simplify the sample fabrication process and suppress the effect of surface modification by an additional wet process. In both cases, the GaN surface was a Ga-terminated (0001) plane (+*c* plane).

The film and bulk GaN samples were rinsed sequentially with acetone and ethanol. One group of samples had no Pt layer (hereafter, "Bare-GaN"). The other samples had a layer of Pt deposited before the gas annealing process (hereafter, "Pt-GaN"). For HAXPES measurements, a 5 or 10 nm-thick Pt layer was uniformly deposited over the entire GaN surface. For electrical measurements, after wet cleaning, a 12 nm-thick Ti/100 nm-thick Pt stacked ohmic electrode was formed on the backside by DC sputtering, followed by annealing at 350 °C for 30 min under N_2 atmosphere. Then, a Pt top electrode with a diameter of 110 μm and a thickness of 250 nm was formed by DC sputtering with a metal mask. Some samples were annealed at 250 °C for 120 s under 30 kPa with the FNO gas diluted to 2% with N_2 gas (hereafter, "FNO-treated"). In the case of the sample for electrical measurement, the back electrode surface was in contact with the susceptor surface of the heat treatment system during the FNO gas treatment. Current–voltage (*I*–*V*) measurements were performed using a semiconductor parameter analyzer (Keysight Technologies, B1500A).

PES was used to study the chemical bonding in the samples. The layers were nondestructively characterized from the surface to the interface using SXPES (Thermo Scientific Sigma Probe) and HAXPES. HAXPES measurements were performed at the BL15XU undulator beamline of SPring-8 using a high-resolution hemispherical electron analyzer (VG Scienta R4000). Details of the HAXPES experimental setup are described elsewhere.[22,23] The total energy resolutions of the SXPES and HAXPES measurements were set to 700 and 240 meV, respectively. The binding energies were calibrated from the Au $4f_{7/2}$ photoelectron peak (84.0 eV) for an Au film placed at the same electrical ground level as the sample. The KolXPD program[24] was used for curve fitting and analysis with the Voigt function (KolXPD's implementation of a pseudo-Voigt profile[21,25]) after Shirley-type background subtraction.[26] For the Pt-deposited samples, charge correction was also performed by fitting the Pt $4f_{7/2}$ peak with a Doniach–Šunjić function[27] after subtracting the Shirley-type background and adjusting its peak binding energy to 71.2 eV.[28,29] The surface morphology was observed by atomic force microscopy (AFM; Hitachi High-Technologies, AFM5000II).

III. RESULTS AND DISCUSSION

A. Bare-GaN

Figure 1 shows the surface morphologies of FNO-treated and untreated Bare-GaN. After the FNO-treatment, the atomic-scale step and terrace structures were maintained, but an increase in surface roughness was observed. In the 2 μm scan area of the AFM images, the root mean square (RMS) roughness value increased from 0.20 nm (Bare-GaN) to 0.32 nm (FNO-treated GaN). The FNO-treated Bare-GaN showed mainly small particles on the edges of terrace structures, which might indicate reactions such as etching by F-based gas treatment.[30]

Figure 2 compares the HAXPES F 1*s*, Ga $2p_{3/2}$, N 1*s*, and O 1*s* spectra of the FNO-treated and untreated Bare-GaN samples. The spectrum of the FNO-treated Bare-GaN shows GaF_x and GaF_3 bonding states [Fig. 2(a)], similar to the results in our previous report on the treatment of GaN with NF_3 gas.[16] Bermudez investigated the bonding states in the reaction of XeF_2 with GaN surfaces[17] and described the influence of band bending and the chemical shift of the Ga 3*d* peak due to GaF_x ($x = 1, 2, 3$) formation. To our knowledge, the literature on fluorinated GaN is insufficient to determine the degree of fluorination based on chemical shifts. The two F 1*s* peaks observed in the spectra collected in the present study could indicate either of species represented as GaF, GaF_2, or GaF_3; the energy positions of the GaF and GaF_2 peaks are similar, complicating attempts to distinguish between these species or determine whether one of the species is absent due to instability or desorption. A comparison of the results presented in the present

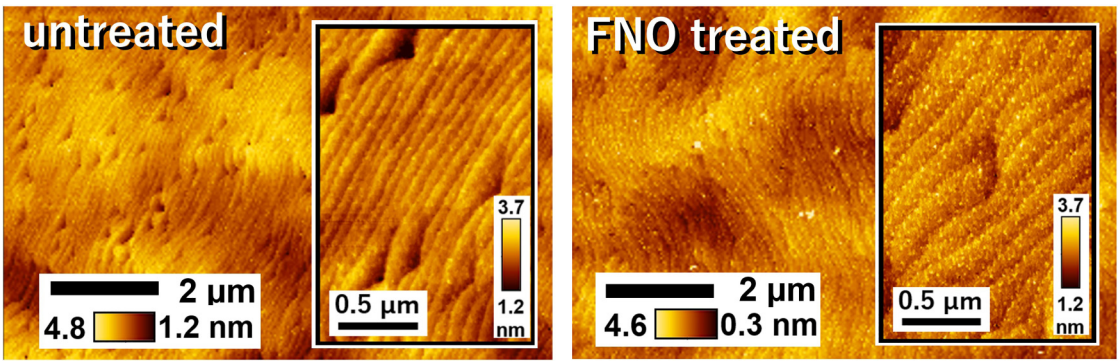

FIG. 1. AFM images of FNO-treated and untreated Bare-GaN. The insets are enlarged images.

study with previously reported results suggests that the high-binding energy side corresponds to GaF_3 and the low-binding energy side corresponds primarily to GaF. For the Ga $2p_{3/2}$ peak in Fig. 2(b), the corresponding bonding state of Ga–F and/or GaO can also be confirmed on the high-binding energy side, which shows a small intensity change after the FNO treatment and is likely due to band bending; the effect of band bending on the shape of N 1*s* peak is not clear [Fig. 2(c) and Fig. S1(a) in the supplementary material]. GaF_x is expected to include a small number of oxidized structures. Residual oxygen is present in the substitution reaction involving FNO. The O 1*s* spectrum [Fig. 2(d)] confirms the presence of three O bonding states. The influence of the surface adsorption layer (–OH) remains in the tail state at ~533.5 eV; the intensity of this peak was reduced after the FNO treatment, whereas that at the low-binding energy side tended to increase. The middle peak corresponds to the GaO_x bonding state. The lowest binding energy side corresponds to the binding states of the oxynitride layer, which might contain F, although its exact composition is difficult to determine. The N peak obscures the other peaks. These changes have been confirmed by both SXPES and HAXPES at depths greater than a few nanometers from the surface (Figs. S1 and S2 in the supplementary material). Basically, a natural oxide film is formed on the GaN surface. This oxide film has been reported to be an ultra-thin GaO_x layer;[31] however, it is responsible for parasitic resistance at the electrode interface and Schottky junction, leading to a reduction of the ON current because of increased series resistance during ON operation, which adversely affects the ON–OFF ratio and reduces the operating voltage.

In addition, in Fig. 2, the Ga $2p_{3/2}$ and N 1*s* peaks in the spectrum of the FNO-treated Bare-GaN sample are shifted to lower binding energy. On the basis of the above assignment, these shifts indicate a shift of the valence band toward the Fermi level. To discuss the valence-band structures for the FNO-treated and untreated Bare-GaN samples, we present the acquired valence-band spectra and a band diagram of the region near the Fermi level, E_F, in Fig. 3. A shift of the valence-band maximum (E_{VBM}) toward the E_F direction is observed [Fig. 3(b)], indicating electron depletion at the surface; in addition, changes are observed in the gap region and the spectral shapes of the valence band. Comparing the edges of the bands reveals that the tail extending toward E_F is more pronounced in the spectrum of the FNO-treated sample than in the spectrum of the untreated sample [Fig. 3(b)], which was pronounced at the surface and confirmed by SXPES. These data suggest an increase in the density of electronic states in the gap. Changes in the spectral shape of the valence band suggest a change in the surface termination. GaN has a hexagonal structure, asymmetric in the ⟨0001⟩ direction, and the termination plane has a Ga or N face. These GaN surfaces strongly affects the valence-band spectral shape.[32–34] The relative intensities of the structures located at the middle and lower binding energies in the valence-band spectrum of the GaN thin film [labeled as P_1 (~5.0 eV), P_2 (~7.8 eV), and P_3 (~10.0 eV) in Fig. 3(a)] are sensitive to the GaN surfaces. Ohsawa *et al.* reported that the P_1 peak for Ga-terminated GaN is more intense than the P_2 peak in HAXPES spectra acquired at $h\nu = 6$ keV, whereas the P_1 peak for N-terminated GaN is weaker than the P_2 peak, which is consistent with the results calculated by using *ab initio* calculations based on density functional theory (DFT).[34] They also reported that the intensity of peak P_3 decreases relative to that of peak P_2 in the spectrum of N-terminated GaN.[30] Typically, Ga-terminated surfaces are formed by metal–organic chemical vapor deposition (MOCVD) of GaN onto a sapphire substrate. However, since the XPS results include information several atomic layers deeper than the top surface, they may not correctly reflect the structure of the top surface in atomic layers due to defects. On the other hand, we have previously compared results of time-of-flight low-energy atom scattering spectroscopy (TOFLAS), which are more sensitive to the topmost atomic layer, with XPS results; in which we found that the surface structure was modified by defect structures, but the tendency for the P_1 to be stronger is consistent due to the Ga surface.[35] In the present study, the intensity of the P_1 peak is reduced to the same level as that of the P_2 peak in the FNO-treated samples. This decrease in peak intensity is inconsistent with a Ga-terminated structure and suggests a change in surface termination.

Collectively, the core-level spectra indicate that fluorination in GaN by the FNO treatment could proceed as follows: The Ga-terminated structure ideally has dangling bonds at the surface. The FNO treatment acts upon the bonds, terminating them with F and resulting in a GaF_3 structure. Other bonding states

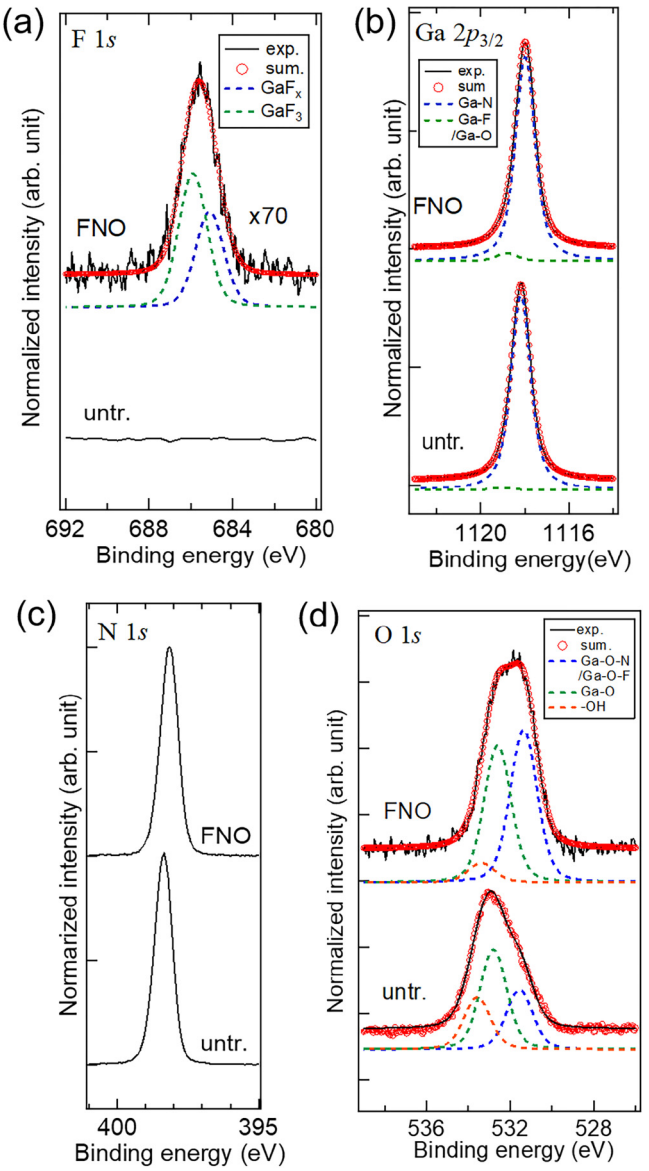

FIG. 2. (a) F 1s, (b) Ga $2p_{3/2}$, (c) N 1s, and (d) O 1s core-level spectra for FNO-treated and untreated Bare-GaN. The solid lines are the experimental data, the dashed lines are the Voigt profiles, and the red dots are their sum.

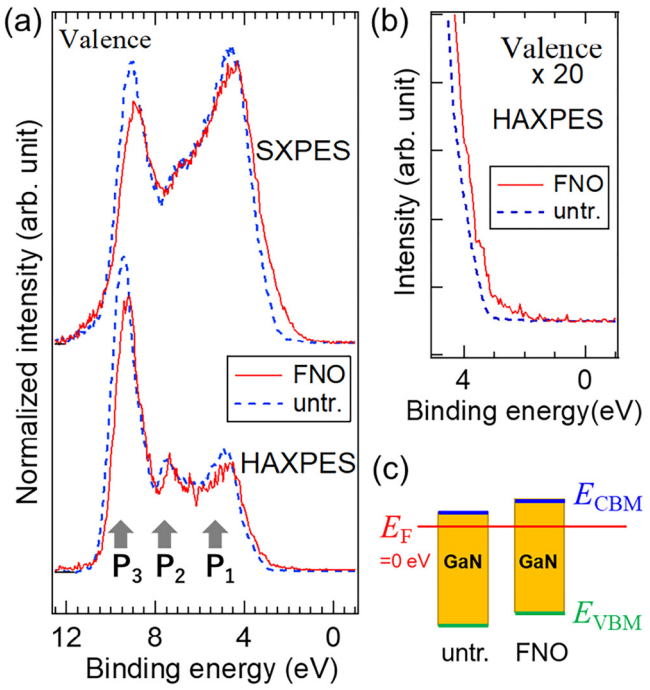

FIG. 3. (a) Valence-region spectra for FNO-treated and untreated Bare-GaN, as obtained by SXPES and HAXPES. The binding energy of 0 eV is the Fermi level (E_F). (b) Magnified spectra corresponding to the Fermi level. (c) Schematics of the Fermi level position in FNO-treated and untreated Bare-GaN.

can exist, such F interstitials caused by defects in GaN or by surface oxidization. Possible defects include through-dislocations, as observed by AFM, and irregular structures resulting from inadvertent surface oxidation. However, these results show that the incorporation of F slightly increased the density of gap states rather than passivating and oxidizing them. We reported in the present study that the Pt/GaN stacking structure reduces the effect of strong fluorination and induces additional reactions. To identify the effect of strong fluorination in the FNO-treated Pt/GaN samples, we investigated their Pt/GaN stacking structure.

B. Pt-GaN

Figure 4 compares F 1s, Ga $2p_{3/2}$, O 1s, and Pt 4f spectra obtained by HAXPES analysis of the FNO-treated and untreated Pt-GaN samples. The F 1s peak appears in the FNO-treated 5 nm-thick Pt-GaN sample. The GaF_3-to-GaF_x intensity ratio increased compared with that of FNO-treated Bare-GaN. By contrast, in the FNO-treated 10 nm-thick Pt-GaN sample, in the current measurement setup, the target peak seems to be present, but no clear intensity was obtained for the background noise of the measurement. There is a possible explanation for these changes of peaks owing to the probing depth of our HAXPES measurement. For Pt, the inelastic mean free path (IMFP[20]) of Pt $4f_{7/2}$ for HAXPES is 4.68 nm, and the probing depth is approximately 15 nm (probing depth: 3× IMFP[21]) below the surface in our experimental setup. However, since the detected signal intensity decreases exponentially, it decreased by more than two orders of magnitude at 5 and 10 nm, and it is considered that it could not be detected at 10 nm under the present measurement conditions because it was at 5 nm and required a long integration time. Given that the intensity of the standardized peak for N in the Pt-GaN sample increased compared with that for N in the Bare-GaN sample and that the

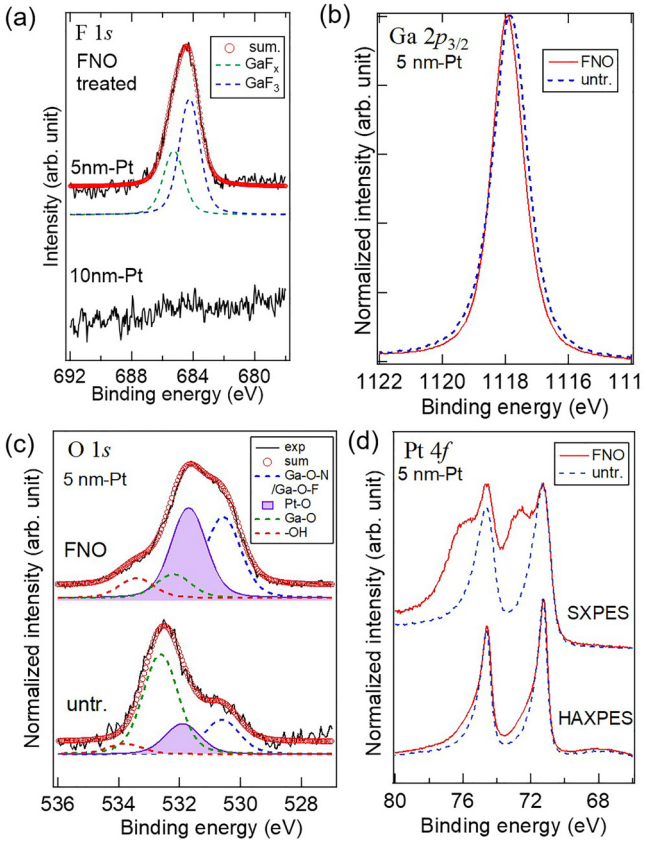

FIG. 4. (a) F 1*s*, (b) Ga 2$p_{3/2}$, (c) O 1s, and Pt 4*f* core-level spectra for FNO-treated and untreated Pt-GaN. The solid lines are the experimental data, the dashed lines are the Voigt profiles, and the red dots are their sum.

detection depth in Bare-GaN was slightly larger at the GaN surface than that in Pt-GaN, and F is present in a very thin region near the interface between the GaN surface and the Pt layer. In the Ga 2$p_{3/2}$ spectrum corresponding to the GaN side after Pt layer formation, the peak shifts by ∼0.5 eV to higher binding energy compared with the corresponding peak in the Ga 2$p_{3/2}$ spectrum of the untreated Bare-GaN, irrespective of the gas treatment. This trend is similar to that observed in the N 1*s* spectra [Fig. S3(a) in the supplementary material], indicating that the formation of the Pt junction shifts the Fermi level to the in-gap region and suggesting that depletion occurs at the interface side, accompanied by the formation of a Schottky barrier. In addition, the full width at half-maximum (FWHM) of the Ga 2$p_{3/2}$ peak at ∼1118 eV is reduced by 0.1 eV [Fig. S3(b) in the supplementary material], suggesting that oxide layer reduction and compensation of defective layers are occurring near the interface. In the Ga spectrum of Bare-GaN, the FWHM of the main peak does not increase because of the change in GaON; by contrast, in the spectrum of Pt, the FWHM changes. In this regard, we focused on the O 1*s* spectra.

Figure 4(c) shows the results of peak fitting of the O 1*s* spectrum after the Pt 3*p* and background data were subtracted from the acquired data [original data are shown in the Fig. S4(a) in the supplementary material]. The formation of Pt–O is also confirmed by the Pt 4*f* spectra, as shown in Fig. 4(d) [fitted data are shown in Fig. S4(b) in the supplementary material]. In the spectra of FNO-treated Bare-GaN, core-level peaks related to Ga–O, OH, and GaO–F or GaO–N bonding states are observed in the O 1*s* region [Fig. 2(d)]; by contrast, for FNO-treated Pt/GaN, an additional peak observed at ∼532 eV in the spectra is attributed to a core-level peak derived from Pt–O.[36] In some cases, a small amount of Pt–O is formed at the Pt/oxide interface and deformation is observed on the high-binding energy side of the Pt 4*f* spectrum, where peaks associated with metallic Pt 4$f_{7/2}$ and 4$f_{5/2}$ overlap, indicating Pt–O formation. However, evidence of the formation of Pt–O was not observed in the spectrum of untreated Pt/GaN. The formation of PtO_x is considered to be more closely related to the redox process at the GaN interface than to the uptake of oxygen from FNO gas during the post-treatment process. In the O 1*s* region, the peak intensity ratio clearly changes, confirming the phenomenon observed for the Ga–O peak and the increase in the Pt–O peak intensity. An increase in peak intensity at low binding energy is also observed; however, it is attributable to residual elements from fluorination, as was the case with Bare-GaN. At the Pt/GaO_x interface, a catalytic effect is expected, and NO desorption is induced.[37,38] In addition, the formation of PtO_2 is promoted,[39] albeit at a high temperature relative to that used in the present experiment. This catalytic effect is speculated to have led to decomposition of FNO, reduction of GaO_x near the interface, and fluorination of the resultant reduced Ga. On the basis of the above discussion, fluorination during the FNO gas treatment might be effectively promoted by a combination of metals expected to have a catalytic effect. Note that this Pt 4*f* change was also observed in the FNO-treated 10 nm-thick Pt-GaN sample; furthermore, our previous results indicate that due to the columnar structure of Pt, fluorine-based gas (NF_3 gas) can penetrate into the Pt layer.[16] In contrast to the NF_3 gas, the fluorination ability of FNO gas is weaker than that of NF_3 gas, so the fluorination of Pt and GaN (F 1*s* signal) in the FNO-treated 10 nm-thick Pt-GaN sample was not clearly observed. The HAXPES results are simply summarized in Table S1 in the supplementary material.

C. Electrical properties

The FNO gas treatment is expected to improve the Pt/GaN interface by reducing the remaining GaO_x interfacial bonds. Although the Pt layer is partly oxidized, the spectral changes for Pt before and after treatment suggest that the Pt layer containing oxidized Pt retains its electrode function. Because the reduction effect occurring at the GaN interface can enhance the Schottky contact properties, we fabricated and evaluated Schottky junctions. Figure 5(a) shows *I*–*V* curves at the voltage from −5 to 5 V for the untreated and FNO-treated Pt/GaN samples. The increase in current with forward voltage is approximately three orders of magnitude higher for the FNO-treated sample than for the untreated sample. Although the effect of the FNO gas treatment on back contact should also be considered, it is also thought that the decrease in the number of Ga–O bonds at the interface, as confirmed

by HAXPES analysis, is also having an effect. The ON–OFF ratio increased because of the higher forward current.

To investigate the Schottky barrier height in detail, we analyzed the I–V characteristics using thermal electron emission theoretical Eqs. (1) and (2),[40]

$$I = I_S\left\{\exp\left(\frac{qV}{nkT}\right) - 1\right\}, \tag{1}$$

$$I_S = SA^{**}T^2\exp\left(-\frac{q\Phi_B}{kT}\right), \tag{2}$$

where S is the contact area, q is the electronic charge, n is the ideality factor, k is the Boltzmann constant, T is the temperature, Φ_B is the Schottky barrier height, and A^{**} is the effective Richardson constant. The theoretical value of $A^{**} = 32$ A/(cm^2 K^2) was used in the present study.[41] The values of Φ_B for the FNO-treated and untreated samples were obtained as 1.06 and 0.97 eV, which are averaged values obtained from five measurement points on the sample, and their ideality factors were also estimated as 1.11 and 1.28, respectively. The change in barrier height may also be due to the effect of Fermi level pinning. Isobe *et al.* reported that the Fermi level pinning effect is reduced by changes in the oxidation state of the interface, and that this improves the barrier height.[42] The reduction in the oxidation layer at the interface is shown in the XPS results and is in agreement with the experimental results. With respect to the leakage current in the reverse voltage direction up to −100 V, as shown in Fig. 5(b), the FNO-treated samples showed an increase in leakage current of a few digits in the range from −10 to −20 V but showed stable characteristics up to the high voltage range at several measurement points. On the other hand, in the untreated sample, there were measurement points where the leakage current characteristics were lower than those of the FNO-treated sample in the high voltage range, but there was variation in the breakdown voltage. It is thought that the uniformity of the interface is improved by the reduction reaction of the FNO gas treatment, but in the high voltage range, it is believed that the improvement of the interface characteristics by optimizing the processing time, etc., is necessary to suppress leakage. These results suggest that FNO gas treatment has the potential to be an effective post-processing method for improving the interface of Pt/GaN systems.

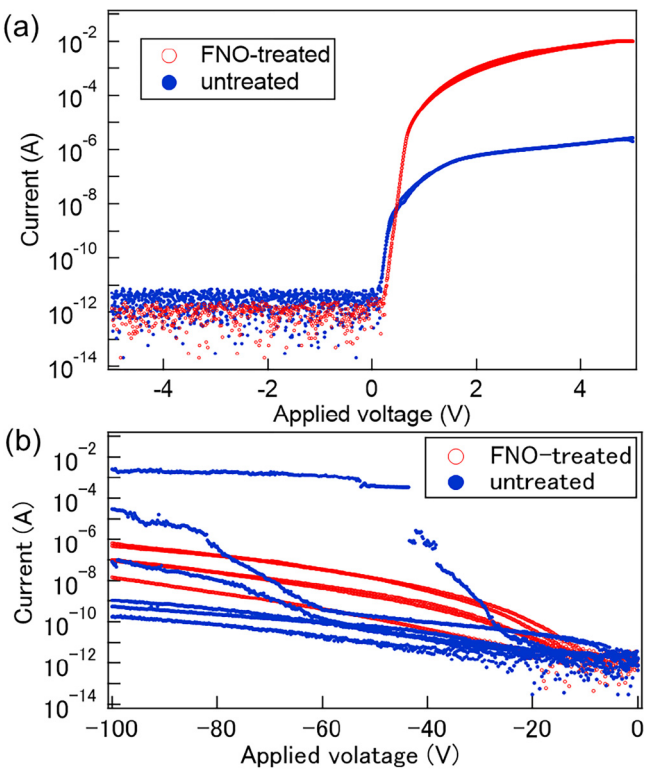

FIG. 5. *I–V* properties (a) from −5 to 5 V and (b) on the reverse bias side of 0 to −100 V of FNO-treated and untreated Pt-GaN.

IV. CONCLUSION

We investigated the effects of FNO gas treatment of GaN and found that FNO is effective in fluorinating its surface, giving rise to a prominent F peak and chemically shifted Ga peaks in the corresponding HAXPES spectra, indicating the formation of GaF_x ($x = 1$, 2, and 3) species. The effects of the FNO treatment were observed not only in Bare-GaN samples but also in Pt/GaN samples treated with FNO after Pt deposition. The Pt/GaN structure showed enhanced redox reactions because of the catalytic effect induced by Pt/GaO; this enhancement was not observed in the case of Bare-GaN. The FNO treatment oxidized the Pt side but reduced the oxide layer on the GaN side, improving its electrical properties. The findings of the present study suggest that FNO treatment is an effective post-processing method for fluorinating GaN-based systems after metal deposition. Moreover, compared with other fluorination methods such as exposure to CF_4 plasma, the proposed method fluorinates the GaN or its metal interface without subjecting the surface to high-energy incident ions and can, therefore, be considered a viable low-damage process.

SUPPLEMENTARY MATERIAL

Figure S1(a) shows the N 1*s* spectra for Bare-GaN. Figure S2 shows F 1*s*, O 1*s*, and Ga $2p_{3/2}$ core-level spectra for Bare-GaN. Figure S3(a) shows N 1*s* spectra of the 5 nm-thick Pt-GaN samples. Figure S4 shows Pt $4p_{3/2}$, O 1*s*, and Pt 4*f* core-level spectra of the 5 nm-thick Pt-GaN samples.

ACKNOWLEDGMENTS

We are grateful to HiSOR, Hiroshima University, and JAEA/SPring-8 for the development of HAXPES at BL15XU of SPring-8. The HAXPES measurements were performed under approval of the NIMS Synchrotron X-ray Station (Proposal Nos. 2016A4600, 2016B4601, 2016B4602, 2017A4604, and 2020A4602). This work was supported in part by JSPS KAKENHI Grant No. 20H02188, "Advanced Research Infrastructure for Materials and Nanotechnology in Japan (ARIM)" of the Ministry of Education,

Culture, Sports, Science and Technology (MEXT), Proposal No. JPMXP1223NM5168.

AUTHOR DECLARATIONS

Conflict of Interest

The authors have no conflicts to disclose.

Author Contributions

Takahiro Nagata: Data curation (lead); Formal analysis (lead); Investigation (lead); Methodology (equal); Project administration (supporting); Writing – original draft (lead); Writing – review & editing (equal). **Asahiko Matsuda:** Data curation (equal); Formal analysis (equal); Investigation (equal); Writing – review & editing (equal). **Takashi Teramoto:** Formal analysis (supporting); Funding acquisition (lead); Investigation (supporting); Methodology (equal); Project administration (supporting); Supervision (equal). **Dominic Gerlach:** Conceptualization (equal); Formal analysis (equal); Investigation (supporting); Methodology (equal); Project administration (lead). **Peng Shen:** Conceptualization (equal); Formal analysis (equal); Investigation (supporting); Methodology (equal); Project administration (lead). **Shigenori Ueda:** Formal analysis (equal); Investigation (equal); Methodology (equal); Writing – review & editing (supporting). **Takako Kimura:** Conceptualization (lead); Formal analysis (equal); Funding acquisition (lead); Investigation (supporting); Methodology (supporting). **Christian Dussarrat:** Conceptualization (lead); Funding acquisition (lead); Investigation (supporting); Methodology (supporting); Supervision (equal). **Toyohiro Chikyow:** Conceptualization (lead); Formal analysis (supporting); Funding acquisition (lead); Investigation (supporting); Methodology (equal); Project administration (supporting); Supervision (equal).

DATA AVAILABILITY

The data that support the findings of this study are available from the corresponding author upon reasonable request.

REFERENCES

[1]S. J. Pearton, J. C. Zolper, R. J. Shul, and F. Ren, "GaN: Processing, defects, and devices," J. Appl. Phys. **86**, 1 (1999).
[2]C. G. Van de Walle, "Energies of various configurations of hydrogen in silicon," Phys. Rev. B **49**, 4579 (1994).
[3]C. G. Van de Walle, "Interactions of hydrogen with native defects in GaN," Phys. Rev. B **56**, R10020 (1997).
[4]B. Szûcs, A. Gali, Z. Hajnal, P. Deák, and C. G. Van de Walle, "Physics and chemistry of hydrogen in the vacancies of semiconductors," Phys. Rev. B **68**, 085202 (2003).
[5]A. Hierro, S. A. Ringel, M. Hansen, J. S. Speck, U. K. Mishra, and S. P. DenBaars, "Hydrogen passivation of deep levels in n–GaN," Appl. Phys. Lett. **77**, 1499 (2000).
[6]X. D. Pi, C. P. Burrows, and P. G. Coleman, "Fluorine in silicon: Diffusion, trapping, and precipitation," Phys. Rev. Lett. **90**, 155901 (2003).
[7]W. S. Jung, J. H. Park, A. Nainani, D. Nam, and K. C. Saraswat, "Fluorine passivation of vacancy defects in bulk germanium for Ge metal-oxide-semiconductor field-effect transistor application," Appl. Phys. Lett. **101**, 072104 (2012).
[8]H. Chen, C. H. Kao, Y. C. Chen, H. K. Lo, Y. M. Yeh, T. C. Lu, H. M. Huang, and C. S. Lai, "Passivation of yellow luminescence defects in GaN film by annealing and CF_4 plasma treatment," J. Optoelectron. Adv. Mater. **13**, 973 (2011).
[9]M. Reiner, P. Lagger, G. Prechtl, P. Steinschifter, R. Pietschnig, D. Pogany, and C. Ostermaier, "Modification of 'native' surface donor states in AlGaN/GaN MIS-HEMTs by fluorination: Perspective for defect engineering," in *2015 IEEE International Electron Devices Meet* (IEDM, 2015), p. 35.5.1.
[10]M. J. Wang, L. Yuan, C. C. Cheng, C. D. Beling, and K. J. Chen, "Defect formation and annealing behaviors of fluorine-implanted GaN layers revealed by positron annihilation spectroscopy," Appl. Phys. Lett. **94**, 061910 (2009).
[11]M. J. Wang, L. Yuan, K. J. Chen, F. J. Xu, and B. Shen, "Diffusion mechanism and the thermal stability of fluorine ions in GaN after ion implantation," J. Appl. Phys. **105**, 083519 (2009).
[12]S. Huang, H. Chen, and K. J. Chen, "Effects of the fluorine plasma treatment on the surface potential and Schottky barrier height of $Al_xGa_{1-x}N$/GaN heterostructures," Appl. Phys. Lett. **96**, 233510 (2010).
[13]K. Orita, M. Kawaguchi, Y. Kawaguchi, S. Takigawa, and D. Ueda, "Efficient outdiffusion of hydrogen from Mg-doped nitrides by NF_3 annealing," J. Electron. Mater. **38**, 538 (2009).
[14]C. Kauppinen, S. A. Khan, J. Sundqvist, D. B. Suyatin, S. Suihkonen, E. I. Kauppinen, and M. Sopanen, "Atomic layer etching of gallium nitride (0001)," J. Vac. Sci. Technol. A **35**, 060603 (2017).
[15]D. C. Messina, K. A. Hatch, S. Vishwakarma, D. J. Smith, Y. Zhao, and R. J. Nemanich, "Challenges in atomic layer etching of gallium nitride using surface oxidation and ligand-exchange," J. Vac. Sci. Technol. A **41**, 022603 (2023).
[16]A. Matsuda, T. Teramoto, T. Nagata, D. Gerlach, P. Shen, S. Ueda, T. Kimura, C. Dussarrat, and T. Chikyow, "NF_3 and F_2 gas fluorination of GaN surface and Pt/GaN interface analyzed by hard X-ray photoelectron spectroscopy," Appl. Surf. Sci. **659**, 159941 (2024).
[17]V. M. Bermudez, "Investigation of the initial chemisorption and reaction of fluorine (XeF_2) with the GaN(0001)-(1 × 1) surface," Appl. Surf. Sci. **119**, 147 (1997).
[18]D. D. Wagman, W. H. Evans, V. B. Parker, R. H. Schumm, I. Halow, S. M. Bailey, K. L. Churney, and R. L. Nuttall, "The NBS tables of chemical thermodynamic properties: Selected values for inorganic and C1 and C2 organic substances in SI units," J. Phys. Chem. Ref. Data **11**(Suppl 2), 67–131 (1982).
[19]A. Kennedy and C. B. Colburn, "Strength of the N–F bonds in NF_3 and of N–F and N–N bonds in N_2F_4," J. Chem. Phys. **35**, 1892 (1961).
[20]S. Tanuma, C. J. Powell, and D. R. Penn, "Calculations of electron inelastic mean free paths. V. Data for 14 organic compounds over the 50–2000 eV range," Surf. Interface Anal. **21**, 165 (1994).
[21]C. J. Powell, A. Jablonski, I. S. Tilinin, S. Tanuma, and D. R. Penn, "Surface sensitivity of auger-electron spectroscopy and X-ray photoelectron spectroscopy," J. Electron Spectrosc. Relat. Phenom. **98–99**, 1 (1999).
[22]S. Ueda, Y. Katsuya, M. Tanaka, H. Yoshikawa, Y. Yamashita, S. Ishimaru, Y. Matsushita, K. Kobayashi, R. Garrett, I. Gentle, K. Nugent, and S. Wilkins, "Present status of the NIMS contract beamline BL15XU at SPring-8," AIP Conf. Proc. **1234**, 403 (2010).
[23]S. Ueda, "Application of hard X-ray photoelectron spectroscopy to electronic structure measurements for various functional materials," J. Electron Spectrosc. Relat. Phenom. **190**, 235 (2013).
[24]J. Libra, KolXPD. Kolibrik.net (2017).
[25]A. Thorne, U. Litzén, and S. Johansson, *Spectrophysics: Principles and Applications* (Springer Science & Business Media, 1999).
[26]D. A. Shirley, "High-Resolution X-Ray photoemission spectrum of the valence bands of gold," Phys. Rev. B **5**, 4709 (1972).
[27]S. Doniach and M. Sunjic, "Many-electron singularity in X-ray photoemission and X-ray line spectra from metals," J. Phys. C **3**, 285 (1970).
[28]J. F. Moulder, W. F. Stickle, P. E. Sobol, and K. D. Bomben, *Handbook of X-Ray Photoelectron Spectroscopy* (Perkin-Elmer, 1992).

[29]"NIST X-Ray Photoelectron Spectroscopy Database," *NIST Standard Reference Database Number 20, Version 4.1* (National Institute of Standards and Technology, 2012).
[30]Y. Youngrak Park, J. Kim, W. Chang, D. Jung, S. Bae, J. Mun, C. H. Jun, S. Ko, and E. Nam, "Normally-off GaN MIS-HEMT using a combination of recessed-gate structure and CF_4 plasma treatment," Phys. Status Solidi A **212**, 1170 (2015).
[31]Y. Irokawa, K. Mitsuishi, T. Nabatame, K. Kimoto, and Y. Koide, "Investigation of intermediate layers in oxides/GaN(0001) by electron microscopy," Jpn. J. Appl. Phys. **57**, 118003 (2018).
[32]T. D. Veal, P. H. Jefferson, L. F. J. Piper, C. F. McConville, T. B. Joyce, P. R. Chalker, L. Considine, H. Lu, and W. J. Schaff, "Transition from electron accumulation to depletion at InGaN surfaces," Appl. Phys. Lett. **89**, 202110 (2006).
[33]G. Martin, S. Strite, A. Botchkarev, A. Agarwal, A. Rockett, H. Morkoç, W. R. L. Lambrecht, and B. Segall, "Valence-band discontinuities of wurtzite GaN, AlN, and InN heterojunctions measured by x-ray photoemission spectroscopy," Appl. Phys. Lett. **65**, 610 (1994).
[34]T. Ohsawa, S. Ueda, M. Suzuki, Y. Tateyama, J. R. Williams, and N. Ohashi, "Investigating crystalline-polarity-dependent electronic structures of GaN by hard x-ray photoemission and ab-initio calculations," Appl. Phys. Lett. **107**, 171604 (2015).
[35]T. Nagata, Y. Suemoto, Y. Ueoka, M. Mesuda, L. Sang, and T. Chikyow, "Polarity control of an all-sputtered epitaxial GaN/AlN/Al film on a Si(111) substrate by intermediate oxidization," ACS Omega **7**, 19380 (2022).
[36]G. M. Bancroft, I. Adams, L. L. Coatsworth, C. D. Bennewitz, J. D. Brown, and W. D. Westwood, "ESCA study of sputtered platinum films," Anal. Chem. **47**, 586 (1975).
[37]F. P. Gortsema and R. H. Toenskoetter, "The chemistry of platinum hexafluoride. I. Reactions with nitric oxide, dinitrogen tetroxide, nitrosyl fluoride, and nitryl fluoride," Inorg. Chem. **5**, 1217 (1966).
[38]A. Kotsifa, D. I. Kondarides, and X. E. Verykios, "Comparative study of the chemisorptive and catalytic properties of supported Pt catalysts related to the selective catalytic reduction of NO by propylene," Appl. Catal. B **72**, 136 (2007).
[39]Y. Xu, J. Chen, X. Yuan, Y. Zhang, J. Yu, H. Liu, M. Cao, X. Fan, H. Lin, and Q. Zhang, "Sintering-Resistant Pt on Ga_2O_3 rods for propane dehydrogenation: The morphology matters," Ind. Eng. Chem. Res. **57**, 13087 (2018).
[40]S. M. Sze, *Physics of Semiconductor Devices*, 2nd ed. (Wiley, 1981).
[41]A. Kumar, S. Arafin, M. C. Amann, and R. Singh, "Temperature dependence of electrical characteristics of Pt/GaN Schottky diode fabricated by UHV e-beam evaporation," Nanoscale Res. Lett. **8**, 481 (2013).
[42]K. Isobe and M. Akazawa, "Effects of surface treatment on Fermi level pinning at metal/GaN interfaces formed on homoepitaxial GaN layers," Jpn. J. Appl. Phys. **59**, 046506 (2020).